

Development and validation of a clinical risk model for postoperative outcome in newly diagnosed glioblastoma: A report of the RANO *resect* group

Philipp Karschnia^o, Jacob S. Young, Gilbert C. Youssef, Antonio Dono^o, Levin Häni, Tommaso Sciortino, Francesco Bruno^o, Stephanie T. Juenger, Nico Teske^o, Jorg Dietrich, Michael Weller^o, Michael A. Vogelbaum, Martin van den Bent, Juergen Beck, Niklas Thon, Jasper K. W. Gerritsen, Shawn Hervey-Jumper^o, Daniel P. Cahill^o, Susan M. Chang, Roberta Rudà, Lorenzo Bello, Oliver Schnell, Yoshua Esquenazi^o, Maximilian I. Ruge^o, Stefan J. Grau, Raymond Y. Huang, Patrick Y. Wen, Mitchel S. Berger^o, Annette M. Molinaro, and Joerg-Christian Tonn^o, on behalf of the RANO Resect Group

All author affiliations are listed at the end of the article

Corresponding Author: Prof. Joerg-Christian Tonn, MD, Department of Neurosurgery, Ludwig-Maximilians-University Munich, Marchioninistrasse 15 / 81377 Munich, Germany (Joerg.Christian.Tonn@med.uni-muenchen.de)

Abstract

Background. Following surgery, patients with newly diagnosed glioblastoma frequently enter clinical trials. Nuanced risk assessment is warranted to reduce imbalances between study arms. Here, we aimed (I) to analyze the interactive effects of residual tumor with clinical and molecular factors on outcome and (II) to define a postoperative risk assessment tool.

Methods. The response assessment in neuro-oncology (RANO) *resect* group retrospectively compiled an international, seven-center training cohort of patients with newly diagnosed glioblastoma. The combined associations of residual tumor with molecular or clinical factors and survival were analyzed, and recursive partitioning analysis was performed for risk modeling. The resulting model was prognostically verified in a separate external validation cohort.

Results. Our training cohort comprised 1003 patients with newly diagnosed isocitrate dehydrogenase-wildtype glioblastoma. Residual tumor, O⁶-methylguanine DNA methyltransferase (*MGMT*) promoter methylation status, age, and postoperative Karnofsky Performance Score were prognostic for survival and incorporated into regression tree analysis. By individually weighting the prognostic factors, an additive score (range, 0–9 points) integrating these four variables distinguished patients with low (0–2 points), intermediate (3–5 points), and high risk (6–9 points) for inferior survival. The prognostic value of our risk model was retained in treatment-based subgroups and confirmed in an external validation cohort of 258 patients with glioblastoma. Compared to previously postulated models, goodness-of-fit measurements were superior for our model.

Conclusions. The novel RANO risk model serves as an easy-to-use, yet highly prognostic tool for postoperative patient stratification prior to further therapy. The model may serve to guide patient management and reduce imbalances between study arms in prospective trials.

Key Points

- Oncological value of resection interacts with other clinical factors.
- Novel RANO risk model integrates the extent of resection with other factors to estimate postoperative survival.
- Goodness-of-fit measurements superior compared to previous risk models.

Importance of the Study

The residual postoperative tumor volume has been associated with survival in newly diagnosed glioblastoma. The interactive effects between the extent of resection and other prognostic factors on outcome are insufficiently understood. We, therefore, studied a molecularly and clinically well-defined cohort of 1003 patients with newly diagnosed IDH-wildtype glioblastoma. Based on this international seven-center cohort, we provide evidence that the association between the extent of resection and outcome depends on other clinical markers. A

novel easy-to-use risk score was designed which integrates residual tumor volume, MGMT promotor status, age, and postoperative KPS to estimate survival on an individual patient level. Given that the prognostic value of the risk model was retained in an external validation cohort of 258 patients with glioblastoma, the novel RANO risk model may serve as a stratification tool to guide therapeutic management and to inform clinical trials, which will eventually help to reduce prognostic imbalances between study arms.

Glioblastoma represents the most frequent primary brain tumor in adults and is characterized by locally destructive infiltrative growth.¹ Maximal safe surgical resection is recommended for initial management of newly diagnosed disease,^{2,3} and in cases where resection appears not safely feasible a biopsy allows for a tissue-based neuropathological diagnosis.⁴ Although surgery is routinely followed by concomitant radiochemotherapy and maintenance chemotherapy, progression inevitably occurs and is characterized by a poor prognosis.⁵ Numerous clinical trials are prospectively enrolling patients with newly diagnosed glioblastoma after initial surgical resection to assess novel medical or radiotherapeutic approaches.^{6,7} Proper risk stratification of enrolled patients prior to randomization is paramount to reduce potential imbalances between study arms, which otherwise might dilute meaningful outcome differences between the interventional and the control arms.

The residual postoperative tumor volume as a measurement for extent of tumor resection has been reliably associated with survival,^{8,9} and we previously established a classification system to standardize terminology across clinical studies (denoted as “*response assessment in neuro-oncology (RANO) categories for extent of resection in glioblastoma*”).¹⁰ Importantly, other clinical predictors of outcome such as neurological function or certain patient demographics have been proposed to interact with the oncological benefits of resection. Nuanced weighting of the oncological role of resection along with these other prognostic factors is warranted to generate a reliable risk stratification system given the heterogenous associations of resection and survival within different clinical or molecular patient subgroups.¹¹

In the current study, we made use of our classification system to analyze the interactive associations of residual tumors with clinical or molecular factors and outcomes in patients with newly diagnosed glioblastoma. The evidence is then compiled into an easy-to-use risk model to estimate the postoperative outcome, and an adjustment for further therapy is applied to retain the prognostic relevance of our risk model independent of therapy after surgery. For that purpose, we also explored whether the prognostic value of the risk model can be verified in an external validation cohort. Finally, we compared our risk model to previously postulated risk models to provide an evidence-based rationale for selecting among the available tools for patient stratification in the setting of prospective clinical trials.

Methods

Clinical data were collected at each study center, and coded data were transferred to the main study center at Ludwig Maximilians University in Munich, Germany. The study protocol including centralized data storage and analysis was approved by the local institutional review board (AZ 21-0996).

Study Population: Training and Validation Cohorts of Newly Diagnosed Glioblastoma

The institutional databases of seven neuro-oncological centers in Europe and the United States were searched for patients with newly diagnosed glioblastoma (Figure 1A). Patients were consecutively treated at the individual institutions and identified based on the following criteria: (I) new tissue-based diagnosis of previously untreated supratentorial isocitrate dehydrogenase (IDH)-wildtype glioblastoma meeting the diagnostic standard stated by the WHO 2021 classification¹²; (II) pre- and postoperative MRI available for review; and (III) follow-up of ≥ 3 months after diagnosis of glioblastoma. In patients meeting the three criteria, a predefined set of demographic, clinical, and tumor volumetric information was extracted from the databases and imaging datasets by the individual study centers. The patients assigned to the training cohort were previously described to establish the classification system for the extent of resection, and a detailed overview of the data stratified per study center was provided.¹⁰ An additional external validation cohort was assembled and has not been previously reported.

Measurements of Tumor Volume for Patient Stratification

For volumetric assessment, tumors were manually delineated on pre- and postoperative scans.^{10,13} Although volumetric measurements were obtained from institutional raters rather than a centralized imaging review, sufficiently low inter-rater variability within our group was previously verified.¹⁰ Whenever possible, postoperative MRI was obtained within 72 h following resection.¹⁴ The total



Figure 1. Baseline characteristics of patients with newly diagnosed glioblastoma assigned to the training cohorts. (A) Geographic representation of the seven neuro-oncological centers providing the training cohort (n = 1003) and the neuro-oncological center providing the training cohort (n = 258). (B) RANO classification for extent of resection in glioblastoma characterizing four distinct classes based upon residual tumor. (C) Distribution of RANO classes, MGMT promoter methylation status, and postoperative therapies across patients assigned to the training cohort. (D) Multivariate analysis for the training cohort using a Cox proportional hazard regression model estimating the hazard ratio for death. All included variables were of significance on univariate analysis. CE: contrast-enhancing; KPS: Karnofsky performance status. Hazard ratio ± 95% confidence interval.

contrast-enhancing tumor was quantified on contrast-enhanced T1-sequences, and non-contrast-enhancing tumor was measured on FLAIR- or T2-sequences.¹⁰ To distinguish non-contrast-enhancing tumor from edema or postsurgical changes, the anatomical tissue integrity of the surrounding parenchyma together with the signal intensity compared to cerebrospinal fluid or normal white matter was considered as recently outlined and proven to be of prognostic relevance.^{4,10,13} Also, other standard-of-care sequences (including non-enhanced T1-sequences) were reviewed to delineate hematoma from residual tumor. Moreover, raters ensured that postoperative FLAIR- or T2-abnormalities were not due to ischemic changes. For this purpose, diffusion-weighted images were utilized when deemed necessary by the raters. For multifocal disease, the volumetrics of each focus were summed together. Absolute tumor volumes measured in cm³ were determined and patients were stratified following the RANO classification for extent of resection. Here, four prognostically distinct classes are distinguished based on the residual tumor volume (Figure 1B).¹⁰ For the validation cohort from the Massachusetts General Brigham network (including Dana–Farber Cancer Institute), only information about a patient's RANO class for the extent of resection but no detailed volumetric details were available for our review.

Definition of Clinical Endpoints

Patients were followed until death or date of database closure, with patients lost to follow-up being censored on the day of the last follow-up. Database closure was in February 2022 for the training cohort, and March 2023 for the validation cohort. Date of surgery (or biopsy if no open resection was performed) was set as date of diagnosis. To avoid overlap with a previously reported cohort from UCSF in which resection was provided between 1997 and 2017,⁸ only UCSF patients in which initial surgery was performed after 2016 were included in the current study. The first MRI showing disease progression per RANO criteria was set as date of first recurrence.¹⁵ While a small subset of patients was evaluated using iRANO/mRANO criteria in the setting of clinical trials, this might not have confounded our analysis given that there is no difference in correlation with outcome compared to the RANO criteria.¹⁶ Progression-free survival was defined as the time between diagnosis and first recurrence or death from any cause, and overall survival was defined as the time between diagnosis and death from any cause.

Statistics: Descriptive Statistics, Risk Modeling, and Validation of the Risk Model

Continuous variables were analyzed for normal distribution and equal variance by making use of the D'Agostino-Pearson test. The unpaired Student's *t*-test was applied to test for differences between two groups with parametric data, and the Mann–Whitney U-test was applied for non-parametric data. Data are expressed as mean ± SEM if not indicated otherwise, and range is given. The relationship between the categorical variables of the two groups

was analyzed using the χ^2 -test, and such variables are described in absolute numbers and percentages.

For survival analysis stratifying two groups to a binary variable, Kaplan–Meier survival estimates and log-rank tests were computed. The proportional hazard assumption was confirmed using scaled Schoenfeld residuals (*versus* time) and deviance residuals. For the calculation of the median follow-up, the reverse Kaplan–Meier method was applied. For univariable survival analysis of outcomes depending on a continuous variable such as age, Cox proportional hazard regression models were calculated to estimate hazard ratios (HRs) and 95% confidence intervals (CIs). Markers of prognostic significance with a *P*-value ≤ 0.05 on univariate analysis were forwarded into a multivariable survival analysis using a Cox proportional hazard regression model.

To analyze the interactive associations of the extent of resection (measured as residual tumor) with other prognostic molecular or clinical factors and survival, recursive partitioning analysis divided the training cohort into different survival risk categories via the Stata model for the CART algorithm.¹⁷ Here, the response to one input variable depends on values of inputs higher in the tree. As such, the hierarchical structure of the decision-tree guarantees that interactions between predictors are automatically modeled.¹⁸ Since residual tumor volume, age, O⁶-methylguanine DNA methyltransferase (MGMT) promoter methylation status, and postoperative Karnofsky Performance Score (KPS) were found to be independently significant by multivariable analysis, they were included as potential splits in the decision tree. Age and postoperative KPS were dichotomized as binary variables by choosing clinically meaningful cut-offs (age: ≤ 65 years as characteristic age defining elderly populations in study protocols¹⁹; postoperative KPS: ≥ 80 with ability to pursue normal activity including work), which proved to be of significance on step-wise log-rank testing. Patients with incomplete information on those variables were dropped by the CART algorithm. The minimal number of events per node was set to 10 deceased patients, and splits are determined by martingale residuals of a Cox model to calculate (approximate) chi-square values for possible cut-points of the covariates. Given that we aimed to construct a postoperative risk model at a time before further therapy had been administered while the use of more aggressive postoperative therapy was significant on multivariate analysis, we performed adjustment of our recursive partitioning analysis for postoperative therapy by incorporation of “postoperative therapy” as a categorical variable in the Stata module for the CART algorithm. Terminal regression tree nodes were integrated into a single risk category if they did not differ when tested by log-rank survival analysis. To translate the resulting risk categories into a clinically easy-to-use risk model, we calculated an additive scoring system that represents the individual risk categories based on the absolute number of points. Points assigned for individual categories reflect the interactions predicted by the decision-tree analysis, and the score reflects the risk categories from the decision-tree analysis. The prognostic value of our calculated risk model was tested in an external validation cohort. Goodness-of-fit measurements (including Harrell's c-index, pseudo-*R*² values, and the index

of prediction accuracy (IPA)) were compared between our risk model and previously postulated models.^{20,21} For calculation of the IPA, model Brier scores (at 18 months following diagnosis) and null model Brier scores were computed using the Stata model for risk prediction in survival analysis.²²

The statistical analyses were performed using Prism (v10.2.1; GraphPad Software Inc., San Diego, CA) and Stata statistical software (v17.0; StataCorp LLC., College Station, TX). The significance level was set at $P \leq 0.05$.

Data Availability Statement

Coded data can be accessed upon qualified request from the corresponding authors.

Results

Baseline Patient Characteristics: Training and Validation Cohorts

Clinical data from 1003 patients with newly diagnosed IDH-wildtype glioblastoma were assembled to serve as a seven-center training cohort, and information from 258 different patients was collected to represent an external single-center validation cohort. All tumors were diagnosed according to the criteria proposed by the WHO 2021 classification based on tissue-based neuropathological assessment.¹² In the entire cohort of 1261 (training and validation) patients, the reported method to assess IDH status was next-generation sequencing ($n = 455$, 36.1%), pyrosequencing ($n = 197$, 15.6%), immunohistochemistry combined with pyrosequencing ($n = 112$, 8.9%), immunohistochemistry alone ($n = 171$; 13.6%), PCR ($n = 7$, 0.6%), or not available for our review ($n = 319$, 25.3%).

In the training cohort, resection of the contrast-enhancing and non-contrast-enhancing tumor was characterized as “supramaximal” resection in 157 patients (15.7%; defined as RANO class 1), as “maximal” resection in 477 patients (47.6%; defined as RANO class 2), as “submaximal” resection in 263 patients (26.2%; defined as RANO class 3), and “biopsy” was provided in 106 patients (10.6%; defined as RANO class 4) (Figure 1C). A total of 755 of 897 patients (84.2%) who underwent an open tumor resection received an MRI within 72 h after resection to determine the residual tumor volume. In 156 patients (15.6%), surgical intervention resulted in new postoperative deficits of any kind. The most commonly encountered deficits were hemiparesis (30/156 patients, 19.2%), aphasia (17/156 patients, 10.9%), and visual field deficits (17/156 patients, 10.9%). *MGMT* promotor status was methylated in 456 patients (45.5%), unmethylated in 350 patients (34.9%), and not available in 197 patients (19.6%). Following resection or biopsy, the vast majority of patients received concomitant radiochemotherapy (828 patients; 82.6%).^{2,3} At the time of database closure after a median follow-up time of 38 months, 845 patients (84.3%) were found to have progressive disease and 667 patients (66.5%) were deceased. Median time until first progression was 8 months (CI: 8–9 months), and overall survival was 17 months (CI: 16–18

months). Differences between centers in clinical characteristics as well as outcomes were previously reported in detail.¹⁰

For patients allocated to the validation cohort, there were no differences regarding demographics compared to the training cohort (Table 1). Here, information on the date of postoperative imaging timing was only available in a small subset of 16 patients, in which MRI was obtained within 72 h in 15 patients (93.8%). Compared to patients in the validation cohort, patients in the validation cohort had more favorable clinical features including more frequent presentation of tumors with subcortical anatomical localizations, higher postoperative KPS, smaller contrast-enhancing tumor volumes on preoperative imaging, and a higher rate of postoperative concomitant radiochemotherapy. However, patients in which surgical tumor resection was performed had generally less extensive resection as quantified by the “RANO classification for extent of resection” compared to patients in the training cohort.

Identification of Prognostic Markers in the Training Cohort

To study the interactive associations of the extent of resection with other clinical or molecular markers and outcomes, we first delineated markers of prognostic relevance in the training cohort. For this purpose, we tested a large set of patient characteristics for their associations with overall survival using a univariate analysis (Table 2). The reported method to control for *MGMT* promotor methylation status was pyrosequencing ($n = 774$ patients, 61.4%), methylation-specific PCR combined with Sanger sequencing ($n = 112$ patients, 8.9%), methylation-specific PCR only ($n = 84$ patients, 6.7%), or not available for our review ($n = 291$ patients, 23.1%). Here, the following markers were favorably associated with overall survival: younger age (as continuous variable), methylated *MGMT* promotor methylation status (as binary variable), higher extent of resection per RANO class (as categorical variable), higher postoperative KPS (as continuous variable), superficial anatomical tumor localization (as categorical variable), and more intense first-line therapy following surgical intervention (ie, any radiochemotherapy; as categorical variable). By computing a multivariate Cox proportional hazard regression model, all these markers except tumor localization retained their prognostic significance (Figure 1D). When testing clinically meaningful binary cut-offs for the continuous variables (age: ≤ 65 years as characteristic age defining elderly populations in study protocols¹⁹; postoperative KPS: ≥ 80 with ability to pursue normal activity including work), those cut-offs yielded the greatest HRs between the two resulting groups. Notably, there was a step-wise decrease in the HR for death with lower RANO classes (reflecting more extensive resection) while the associations between outcome and postoperative management were rather inconsistent depending on the exact type of postoperative therapy provided. When postoperative therapy was removed from the multivariate model, the four key prognostic markers (age, *MGMT* promotor methylation status, RANO class, and postoperative KPS)

Table 1. Characteristics for the training and external validation cohort of newly diagnosed IDH-wildtype glioblastoma. Characteristics are given for patients with newly diagnosed IDH-wildtype glioblastoma WHO grade 4 in the training cohort ($n = 1003$), in the external validation cohort ($n = 258$), and the overall cohort ($n = 1261$). Differences between the groups were assessed using the unpaired Student's t -test (for parametric data) or the Mann-Whitney U -test (for non-parametric data) for continuous variables; and categorical variables were assessed by the χ^2 -test. Kaplan-Meier estimates and log-rank testing were used for survival analyses. (Sub-)cortical refers to the cortical grey matter and the subcortical white matter. Deep-seated refers to midline structure involvement (including thalamus, basal ganglia, hypothalamus, and mesencephalon). P -values are given, and asterisks indicate $P \leq 0.05$.

Clinical characteristics		Training cohort	Validation cohort	Total	P -value
Overall		$n = 1,003$	$n = 258$	$n = 1,261$	
Demographics	<i>Age at diagnosis (years; range)</i>	61.6 \pm 0.4 (18–94)	60.9 \pm 0.7 (23–94)	61.4 \pm 0.3 (18–94)	0.187
	<i>M:F ratio</i>	1:0.7	1:0.7	1:0.7	0.546
Clinical markers	<i>Preoperative KPS (median, range)</i>	80 (20–100)	n.a.	-	-
	<i>Postoperative KPS (median, range)</i>	80 (10–100)	90 (50–100)	80 (10–100)	*0.001
	<i>New postoperative deficit (n, %)</i>	156 (15.6%)	n.a.	-	-
IDH status (n, %)	<i>Wildtype</i>	1,003 (100%)	258 (100%)	1,261 (100%)	1.000
	<i>Mutated</i>	0	0	0	
MGMT promotor (n, %)	<i>Methylated</i>	456 (45.5%)	113 (43.8%)	569 (45.1%)	*0.001
	<i>Non-methylated</i>	350 (34.9%)	136 (52.7%)	486 (38.5%)	
	<i>n.a.</i>	197 (19.6%)	9 (3.5%)	206 (16.3%)	
Localization at diagnosis (n, %)	<i>(Sub-)cortical</i>	759 (75.7%)	228 (88.4%)	987 (78.3%)	*0.001
	<i>Deep-seated</i>	123 (12.3%)	14 (5.4%)	137 (10.9%)	
	<i>Multifocal</i>	121 (12.1%)	16 (6.2%)	137 (10.9%)	
	<i>Dominant</i>	505 (50.3%)	133 (51.6%)	638 (50.6%)	*0.001
	<i>Non-dominant</i>	480 (47.9%)	109 (42.3%)	589 (46.7%)	
Tumor volumes (cm³)	<i>n.a.</i>	18 (1.8%)	16 (6.2%)	34 (2.7%)	
	<i>Preoperative CE</i>	32.8 \pm 0.9	14.8 \pm 1.0	29.1 \pm 0.8	*0.001
	<i>Preoperative non-CE</i>	59.0 \pm 1.7	n.a.	-	-
	<i>Postoperative CE</i>	4.1 \pm 0.4	3.9 \pm 0.3	4.1 \pm 0.3	*0.001
	<i>Postoperative non-CE</i>	36.9 \pm 1.2	n.a.	-	-
RANO class for extent of resection	<i>Class 1 ("supramaximal")</i>	157 (15.7%)	11 (4.3%)	168 (13.3%)	*0.001
	<i>Class 2 ("maximal")</i>	477 (47.6%)	51 (19.8%)	528 (41.9%)	
	<i>Class 3 ("submaximal")</i>	263 (26.2%)	180 (69.8%)	443 (35.1%)	
	<i>Class 4 ("biopsy")</i>	106 (10.6%)	16 (6.2%)	122 (9.7%)	
First-line therapy (n, %)	<i>RT only</i>	63 (6.3%)	2 (0.8%)	65 (5.2%)	*0.001
	<i>TMZ/RT \rightarrow TMZ</i>	744 (74.2%)	172 (66.7%)	916 (72.6%)	
	<i>CeTeG</i>	23 (2.3%)	2 (0.8%)	25 (2.0%)	
	<i>TMZ alone</i>	28 (2.8%)	5 (1.9%)	33 (2.6%)	
	<i>TMZ/RT \rightarrow TMZ + experimental drug</i>	61 (6.1%)	77 (29.9%)	138 (10.9%)	
	<i>None or BSC</i>	67 (6.7%)	0	67 (5.3%)	
	<i>n.a.</i>	17 (1.7%)	0	17 (1.4%)	
Outcome	<i>Follow-up (months)</i>	38 (33–45)	39 (33–56)	38 (34–44)	*0.001
	<i>PFS (months)</i>	8 (8–9)	8 (7–9)	8 (8–9)	0.089
	<i>OS (months)</i>	17 (16–18)	20 (18–22)	18 (17–19)	*0.003

Abbreviations: BSC: best supportive care. CeTeG: TMZ + CCNU/RT \rightarrow TMZ + CCNU. CCNU: lomustine. CE: contrast-enhancing tumor. F: female. IDH: Isocitrate dehydrogenase. KPS: Karnofsky performance status. M: male. MGMT: O⁶-methylguanine DNA methyltransferase. n.a.: not available for review. non-CE: non-contrast-enhancing tumor. OS: overall survival. PFS: progression-free survival. RANO: Response Assessment In Neuro-Oncology. RT: radiotherapy. TMZ: temozolomide. -: not applicable.

remained of significance while any trend was lost for the variable denoting tumor localization.

Developing an Integrative Risk Model for Outcome: Decision-Tree Analysis

Based on the training cohort of patients with newly diagnosed glioblastoma, we aimed to construct a postoperative risk model that is prognostic for survival by weighting prognostic clinical and molecular markers. We forwarded the factors that were of significance in multivariate assessment into a recursive partitioning analysis to build an integrative risk model (Figure 2A). Complete information for all selected variables was available in 771 of the 1003 patients (76.9%) assigned to the training cohort, and only those patients were therefore available for decision-tree analysis. To enhance clinical usability by simplification, we used a dichotomized definition of the variables “age” and “postoperative KPS” for splitting the tree. Given that our risk model aimed to serve as a postoperative stratification tool while the type of postoperative therapy was indeed a prognostic marker on multivariate analysis, the type of postoperative management was not included as a covariate but as a stratification factor for the decision tree. Making use of repetitive tree splitting, the presence of 11 terminal leaves was computed (minimal HR: 0.57, maximal HR: 3.92). By post-hoc combination of terminal decision tree leaves with no differences in log-rank survival analysis, three distinct risk categories were identified (Figure 2B):

- Risk category I ($n = 312$; three leaves): patients with any open cytoreductive resection, a postoperative KPS ≥ 80 , methylated *MGMT* promotor (or unmethylated *MGMT* promotor with “supramaximal” resection), and ≤ 65 years (or > 65 years with “supramaximal” or “maximal” resection);
- Risk category II ($n = 348$; five leaves): patients with a postoperative KPS ≥ 80 following “submaximal” resection, methylated *MGMT* promotor, and > 65 years; patients with a postoperative KPS ≥ 80 following “maximal” or “submaximal” resection and unmethylated *MGMT* promotor; patients with a postoperative KPS < 80 following any open cytoreductive resection and ≤ 65 years (or > 65 years with “supramaximal” or “maximal” resection); and patients with a postoperative KPS ≥ 80 following biopsy and ≤ 65 years;
- Risk category III ($n = 111$; three leaves): patients with a KPS < 80 following “submaximal” resection and > 65 years; patients with a biopsy and > 65 years (or ≤ 65 years with a KPS < 80).

Overall survival was most favorable for patients assigned to risk category I, followed by patients in risk category II, while patients in risk category III had the least favorable outcome (24 (CI: 21–27) versus 16 (CI: 15–18) versus 6 (CI: 4–8) months; $P = 0.001$). Similar observations were made when progression-free survival was used as an endpoint, and each of the three risk categories corresponded to distinct outcomes (11 (CI: 10–12) versus 9 (CI: 8–9) versus 3 (CI: 3–4) months; $P = 0.001$). Patients within an individual risk category therefore did not differ in outcome.

Conversion of the Risk Model into an Additive Score

To determine a patient’s individual postoperative risk in a simplified way, we translated the three risk categories into an additive composite score (entitled “RANO risk score for postoperative outcome”). Here, the presence of the four prognostic key factors (RANO class for the extent of resection, postoperative KPS, age, and *MGMT* promotor methylation status) is acknowledged on an individual point scale (Figure 3A). The total score represents the sum of the points which is individually designated to each of the prognostic factors, and ranges from zero to nine points. The factors “age” and “*MGMT* promotor methylation status” are weighted depending on the presence of other risk factors as predicted by the decision-tree analysis. By calculating the total score, patients characterized by a low (0–2 points; risk category I), intermediate (3–5 points; risk category II), and high risk (6–9 points; risk category III) for poor postoperative outcome can be distinguished.

The prognostic value of the three risk categories was conserved in the training cohort subgroup of patients who were homogeneously treated according to the EORTC-NCIC protocol (TMZ/RT→TMZ) (Figure 3B),²³ and this notion held true when only patients with (sub-)cortical tumor localization were included. Also, the prognostic relevance of the risk model was retained in patients who were managed with other therapeutic approaches. In addition, not only the risk category per se but also the absolute point score was associated with the outcome. An exponential increase in HR for death was predicted for each additional point on the risk score as displayed by univariate Cox proportional hazard regression modeling (with the cumulative risk score being considered as continuous variable) (Figure 3C).

External Validation and Comparison with Other Risk Models

To confirm the prognostic relevance of our risk model and minimize the risk that the observed differences in outcome between the risk categories are due to overfitting, we explored whether the prognostic relevance of our risk model holds true in an external dataset. Complete information on the four key variables necessary to calculate our risk model was available in 210 of the 258 patients (81.4%) assigned to the validation cohort (Figure 4A). Reflecting the different clinical characteristics compared to the training cohort (Supplementary Table S1), a lower fraction of patients was assigned to risk category III. Based on these patients, the value of our risk model was substantiated given that the presence of three prognostically distinct classes was detected (Figure 4B). Here, the overall survival of the 54 patients assigned to risk category I was most favorable with 37 (24–79) months, while the 141 patients in risk category II had an intermediate outcome of 19 (CI: 16–20) months, and the 15 patients denoted as risk category III had a poor survival of 11 (CI: 5–17) months ($P = 0.001$). Notably, here we found the prognostic value of our risk model not only retained in the subgroup of patients treated per EORTC-NCIC protocol (even when limited to patients with (sub-)cortical tumor localization; Figure 4C) but also with other management approaches (Figure 4D).

Table 2. Univariate Cox proportional hazard model for patients with newly diagnosed IDH-wildtype glioblastoma from the training cohort. Univariate analysis testing information on tumor volumetrics together with demographic, clinical, and molecular markers using Cox proportional hazard models among patients with newly diagnosed IDH-wildtype glioblastoma assigned to the training cohort ($n = 1003$). Hazard ratio, 95% confidence interval, and P -value are given for analyzed variables. (Sub-)cortical refers to the cortical grey matter and the subcortical white matter. Deep-seated refers to midline structure involvement (including thalamus, basal ganglia, hypothalamus, and mesencephalon). Asterisks indicate $P \leq 0.05$.

Univariate analysis for the training cohort				
Variable	Type of variable	Overall survival		
		Hazard ratio	95% confidence interval	P -value
<i>RANO class</i>				
RANO class (categorical)	1 ("supramaximal")	0.28	0.2–0.4	*0.001
	2 ("maximal")	0.40	0.3–0.5	*0.001
	3 ("submaximal")	0.50	0.4–0.7	*0.001
	4 ("biopsy"; reference level)	–	–	–
RANO class (continuous)	continuous	1.44	1.3–1.6	*0.001
<i>Demographics</i>				
Sex	Male (versus female)	1.01	0.9–1.2	0.065
Age (years)	Continuous (older)	1.03	1.02–1.04	*0.001
	>65 years (versus ≤ 65 years)	1.8	1.5–2.0	*0.001
<i>Clinical markers</i>				
Postoperative KPS	Continuous (higher)	0.98	0.97–0.99	*0.001
	≥ 80 (versus < 80)	0.56	0.5–0.7	*0.001
New postoperative deficit	No (versus yes)	1.12	0.7–1.1	0.264
Tumor localization	Subcortical	0.68	0.5–0.9	*0.001
	Deep-seated	1.06	0.8–1.4	0.689
	Multifocal (reference level)	–	–	–
Affected hemisphere	Dominant (versus non-dominant)	1.01	0.9–1.2	0.840
<i>Molecular markers</i>				
MGMT promotor status	Unmethylated (versus methylated)	1.43	1.2–1.7	*0.001
<i>Management following surgery</i>				
Further first-line therapy	TMZ/RT \rightarrow TMZ + experimental	0.25	0.2–0.4	*0.001
	CeTeG	0.31	0.2–0.6	*0.001
	TMZ/RT \rightarrow TMZ	0.42	0.3–0.6	*0.001
	Radiotherapy only	0.77	0.5–1.2	0.198
	Temozolomide only	0.82	0.5–1.4	0.452
	No further therapy (reference level)	–	–	–

Abbreviations: CeTeG: TMZ + CCNU/RT \rightarrow TMZ + CCNU. KPS: Karnofsky Performance Score. MGMT: O⁶-methylguanine DNA methyltransferase. RANO: Response Assessment In Neuro-Oncology. RT: radiotherapy. TMZ: temozolomide.

Finally, we aimed to put our risk model into the perspective of available tools for patient stratification in the setting of prospective clinical trials by providing a head-to-head comparison with previously postulated risk models for newly diagnosed glioblastoma (Figure 4E). Making use of our training cohort as well as our validation cohort, we computed goodness-of-fit measurements for our risk model, the simplified RTOG RPA model by Li and colleagues (three risk groups),²⁴ the RPA model by Molinaro and colleagues (four risk groups),⁸ and the GBM-molRPA model by Wee and colleagues (three risk groups).²⁵ As indicated by the calculated Harrel's c-indices and supported by the pseudo- R^2 values, our risk model was superior in concordance between predicted with observed survival compared to the three other

risk models. Also, the simplified RTOG RPA model as well as the RPA model proposed by Molinaro and colleagues even failed to discriminate between different risk groups in our cohorts. While both our risk model and the GBM-molRPA distinguished three risk groups characterized by distinct outcomes, the latter model was designed prior to the current WHO 2021 classification with its restriction of the diagnosis of glioblastoma to IDH-wildtype tumors. As one of three groups in the GBM-molRPA model originally compromised mainly patients with IDH-mutant tumors, the application of the GBM-molRPA model to an IDH-wildtype cohort such as ours virtually only distinguished two outcome groups. The findings on most favorable goodness-of-fit measurements for our risk model also held true when

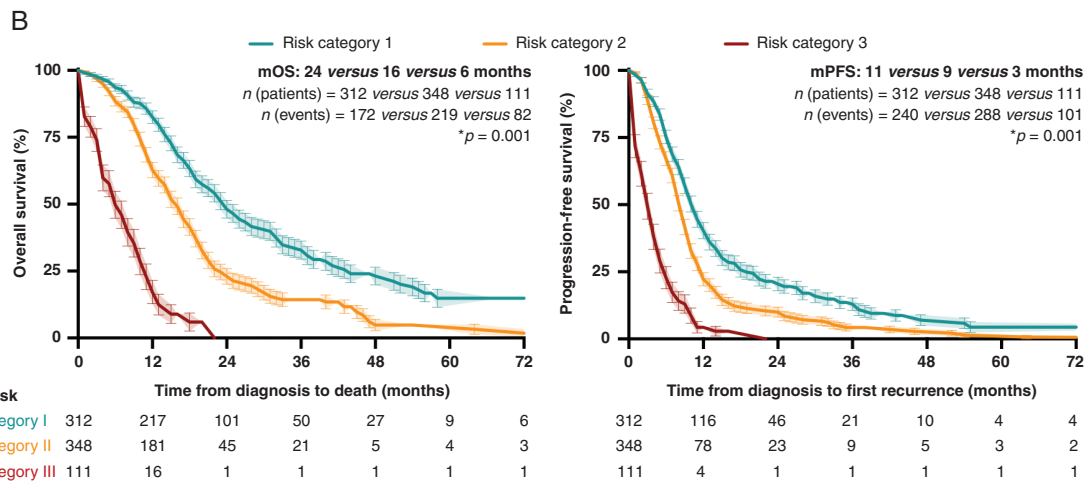
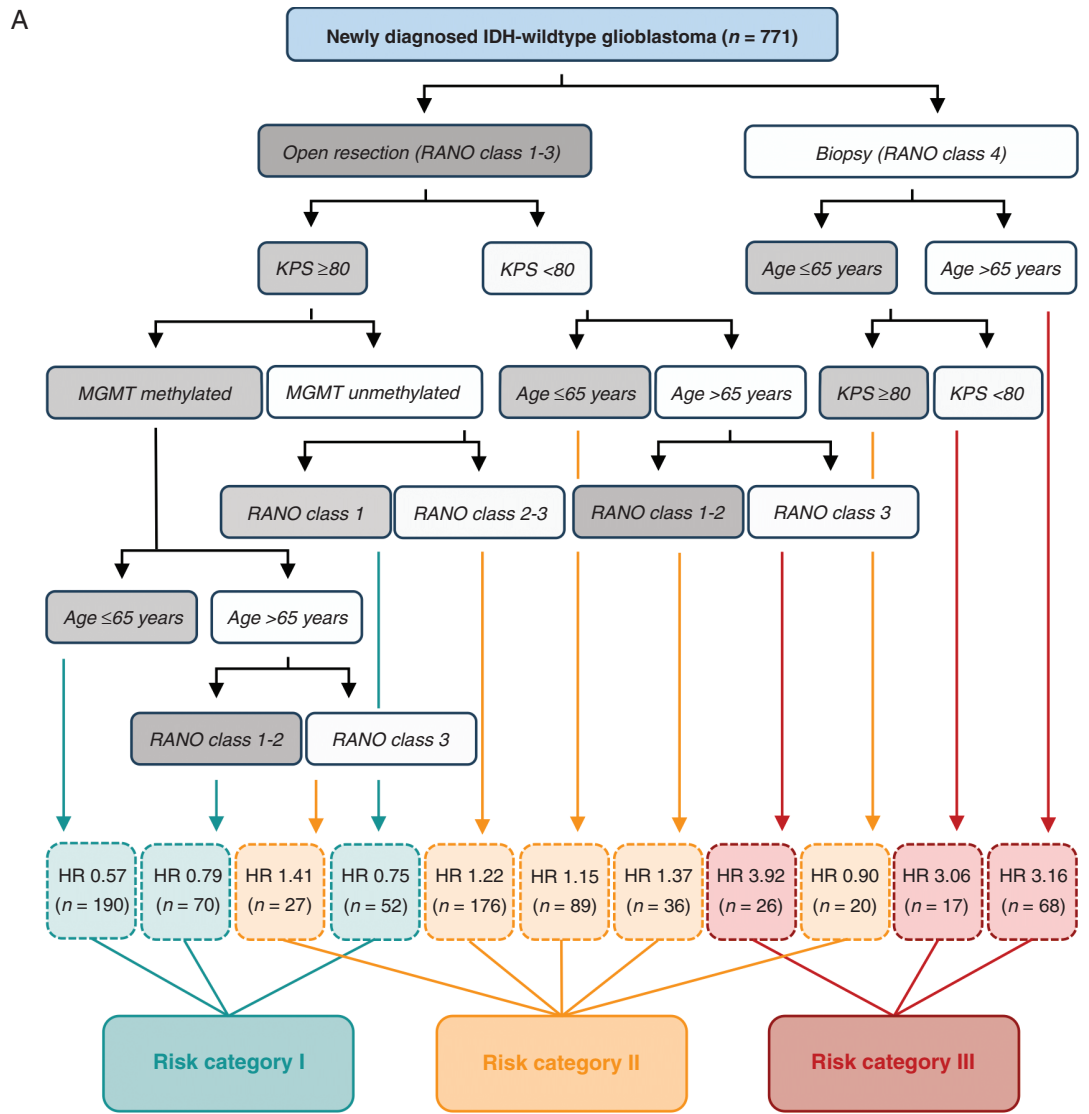


Figure 2. Identification of risk categories by recursive partitioning analysis. (A) Decision-tree analysis for the training cohort integrating the four variables (extent of resection, *MGMT* promoter status, KPS, and age) which were of significance on multivariate analysis. Variables are incorporated as categorical factors, and three distinct risk categories were identified by combination of the terminal decision tree leaves. Note that only patients from the training cohort in which information for all four variables were available were included ($n = 771$), and adjustment for postoperative therapy was applied. Reference to the median overall survival of the training cohort was used by the algorithm. (B) Kaplan–Meier estimates of overall and progression-free survival for training cohort patients stratified to risk category I ($n = 312$) compared to risk category II ($n = 348$) or risk category III ($n = 111$). Points indicate deceased or censored patients, light shading indicates SEM.

the external validation cohort was restricted to the 145 patients in which complete information to calculate all four risk models was available.

Discussion

In 2024, it is expected that more than 12,000 patients will be diagnosed with an IDH-wildtype glioblastoma in the United States.²⁶ Acknowledging the poor median overall survival of 12–17 months,²⁷ novel treatment strategies are desperately needed and clinical trials for innovative therapeutic interventions in addition to radiochemotherapy are regularly offered to affected patients.^{2,3} Based on molecularly well-defined contemporary cohorts of newly diagnosed glioblastoma, we propose a prognostic stratification tool for risk assessment to minimize imbalances between study arms. This easy-to-use risk model exhibits major implications for the design of clinical trials and may guide clinical patient management.

The RANO risk score individually classifies newly diagnosed patients prior to further postoperative therapy as being at low, intermediate, or high risk for poor postoperative survival by integrating clinical and molecular variables into an additive scoring system based on the decision-tree analysis. Given that three distinct survival categories were also observed in the external validation dataset, we ruled out that the prognostic associations of lower scores with more favorable outcomes were induced by the presence of unknown confounders or modeling errors. Our exploratory analysis might implicate associations of higher scores with outcomes even within the same risk category, but the limited sample size does not allow definitive conclusions from such a post-hoc analysis. With the extent of tumor resection being predicted to represent the primary node by recursive partitioning analysis, this points toward a substantial prognostic relevance of resection which corroborates prior findings from prospective trials reporting that patients with lower residual contrast-enhancing tumor volumes experience substantially longer survival.^{28,29} The previously established RANO classification represents an objective and validated tool to quantify the extent of resection,^{10,30–32} and the current data highlight that resection beyond the contrast-enhancing borders might convey an additional survival benefit.⁴ Importantly, both the decision-tree analysis or the risk score might be equally used to assign individual patients to their risk category as the score reflects the results from the recursive partitioning analysis.

Making use of a decision-tree design, our risk model adds granularity to the assumption of a prognostic role for resection by recognizing other prognostic factors such as neurological function,⁹ *MGMT* promotor methylation status,³³ and age.^{19,34} The notion of the interactive effects between risk factors and surgery is exemplified by the salient association of supramaximal resection with outcome in tumors with unmethylated *MGMT* promotor status, while no difference between supramaximal and maximal resection was predicted in patients with methylated *MGMT* promotor status (while both categories being superior to submaximal resection). This finding is in line with prior studies indicating survival benefits of more extensive

resection particularly in unmethylated tumors,²⁸ which might be due to the absence of effects from alkylating chemotherapy to mitigate the unfavorable effects of residual postoperative disease.^{2,3} Importantly, the induction of substantial neurologic deficits may negate the benefit of more extensive resection as acknowledged by our risk model.^{35,36} There was no difference in outcome between older patients in which biopsy was provided compared to older patients in which subtotal open resection with a poor postoperative performance was administered. Here, our data might be interpreted in accordance with the prospective, controlled ANOCEF trial which failed to demonstrate the superiority of open resection over biopsy in individuals over 70 years of age³⁷; and it is tempting to speculate that fewer complete resections in this vulnerable patient cohort might have contributed to the negative results of the ANOCEF trial. In turn, it remains to be seen in future prospective, randomized trials whether a biopsy is per se associated with worse outcomes (compared to subtotal resection) or whether a biopsy is only an indirect surrogate parameter for a less favorable clinical risk profile.

In our two study cohorts, the RANO risk score was superior in predicting accurate outcomes of individual patients compared to other risk models. This might be due to the fact that other models were predominantly developed in the era prior to the WHO 2021 classification,¹² and also due to the detailed integration of the extent of resection into our decision-tree analysis. Further statistical power might be added by determining category-specific cut-offs for continuous variables (including KPS and age) or by the inclusion of in-depth genetic information into the risk model,³⁸ while it will be of importance to conserve simple clinical applicability for routine clinical management and retrospective availability of data to post-hoc assign patients to their risk categories. Although we corrected our statistical approach for further therapy to create a postoperative risk tool, validation in prospective (homogeneously treated) cohorts with a standardized follow-up (imaging) protocol and inclusion criteria (such as tumor localization) is warranted to herald the introduction of our RANO risk score into the design of glioblastoma trials. Given that we did not apply a central slide review in our cohort, we also cannot rule out that a small subset of patients with an H3K27-altered diffuse midline glioma might have been missed. This specifically also includes uncertainty about whether testing for both IDH1 and IDH2 was performed in younger patients, and also which cutoff was applied for *MGMT* methylation status assessment. Acknowledging a high level of surgical neuro-oncological expertise in the contributing study centers, the generalizability of our findings on the prognostic associations with the risk score and outcome to centers with lower case volumes is to be assessed. In this context, more robust yet refined reporting systems for postoperative neurological function are mandatory to be developed.³⁹ Also, data on surgical adjuncts or Carmustine wafer implantation were not available for review as we only controlled for residual tumor volume as a measurement of surgical success. Furthermore, it also remains to be elucidated whether the prognostic value of the risk score is retained in a recurrent disease setting (where supramaximal resection beyond the contrast-enhancing tumor borders might be of less relevance).⁵

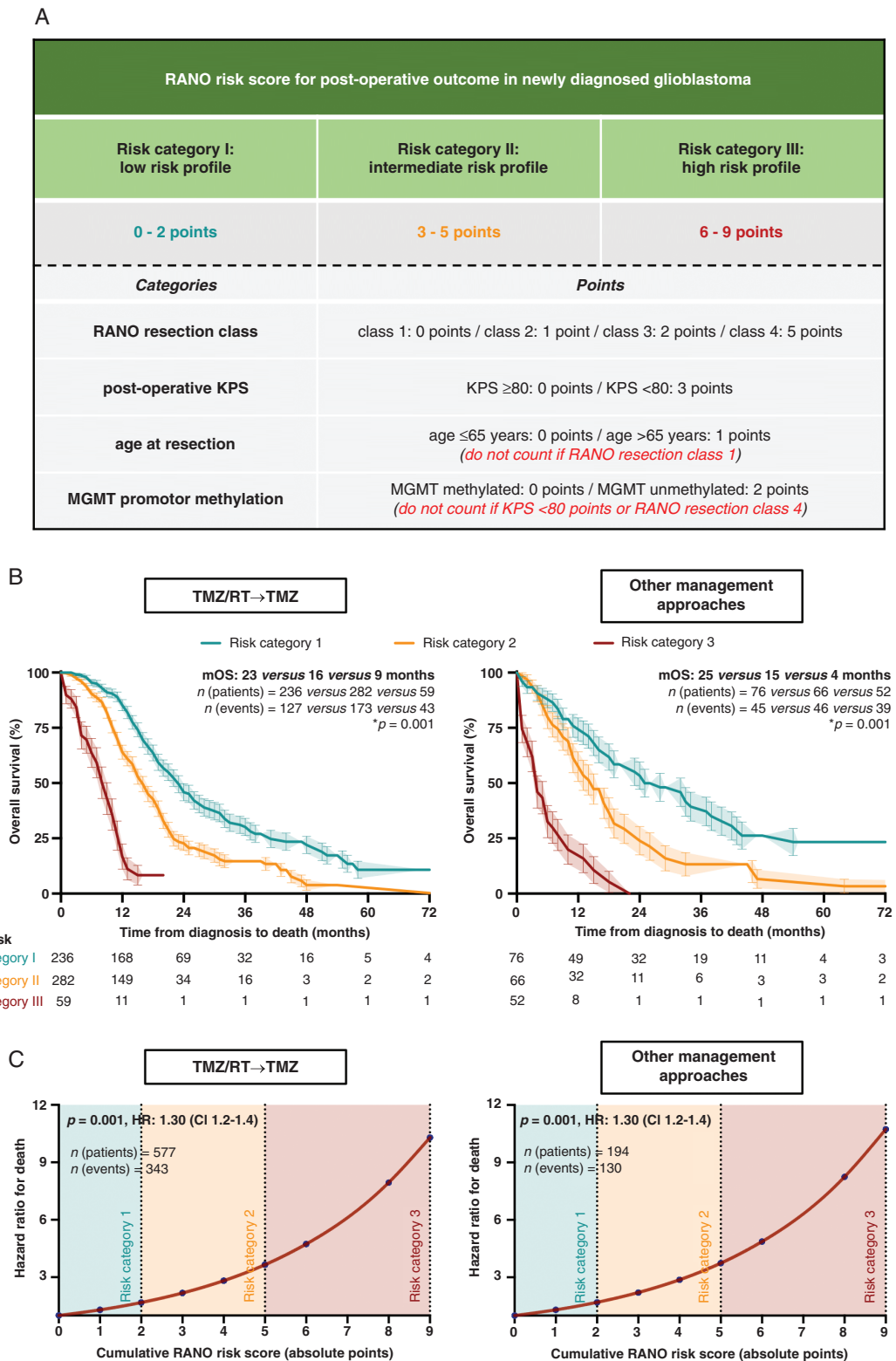
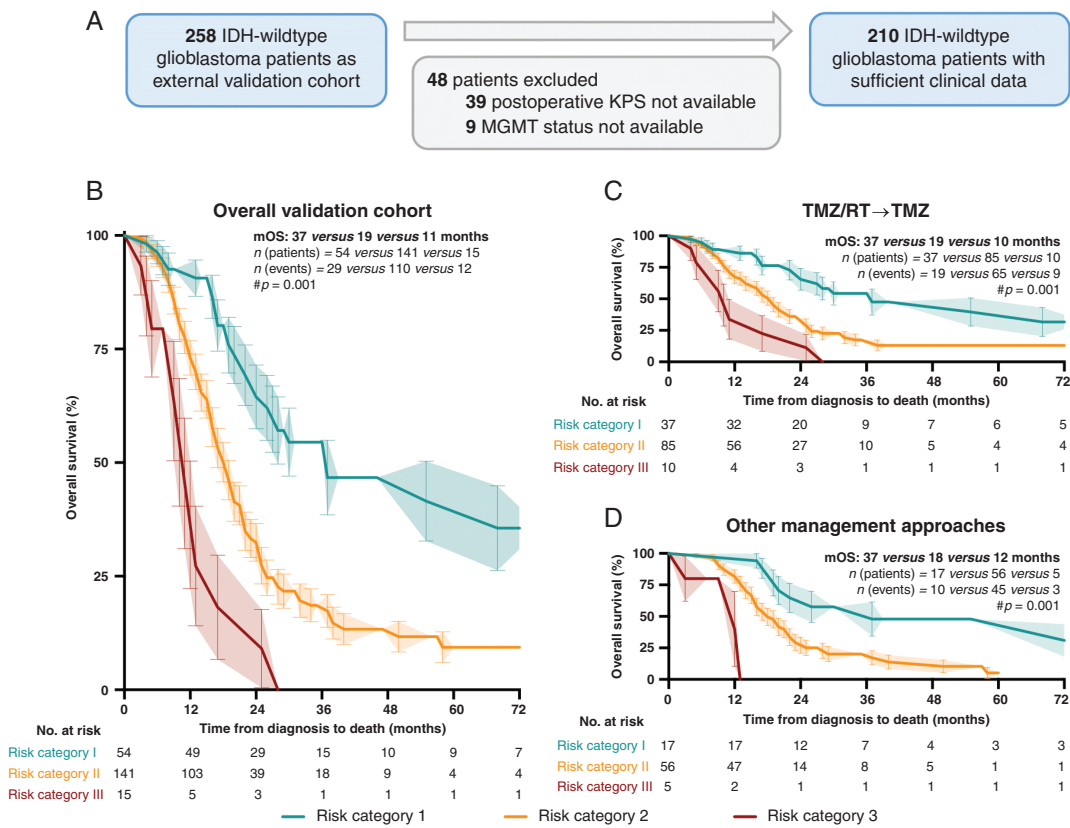


Figure 3. RANO risk score for postoperative outcome. (A) Additive scoring system serving to assign patients to one of the three distinct risk categories based on the total score. Note that each factor is individually weighted, and the individual points dedicated to the two factors *MGMT* promotor status and age depend on the presence of other risk factors. (B) Kaplan–Meier estimates of overall survival for training cohort patients which received postoperative radiochemotherapy (TMZ/RT→TMZ; $n = 577$) or other management approaches ($n = 194$). Patients are stratified into three risk categories based on the RANO risk score, and three prognostically distinct groups can be seen in both patient cohorts. Points indicate deceased or censored patients, light shading indicates SEM. (C) Hazard ratios for death depending on the total score calculated among training cohort patients treated with postoperative radiochemotherapy (TMZ/RT→TMZ; $n = 577$) or other management approaches ($n = 194$). The cumulative RANO risk score was modelled as continuous variable, and an exponential hazard increase can be observed for higher scores.



E

Goodness-of-fit measurements for different risk models								
Risk model (number of groups)	Exploratory cohort (n = 771)				Validation cohort (n = 210)			
	p-value between groups	Harrel's c-index	pseudo-R ²	IPA	p-value between groups	Harrel's c-index	pseudo-R ²	IPA
RANO risk categories (3 groups)	*0.001	0.67 (0.6-0.7)	19.5%	12.8%	*0.001	0.62 (0.6-0.7)	12.6%	11.6%
Simplified RTOG RPA by Li et al. (3 groups)*	*0.001	0.63 (0.6-0.7)	9.6%	8.7%	0.051	0.56 (0.5-0.6)	3.3%	3.3%
RPA by Molinaro et al. (4 groups)	*0.001	0.63 (0.6-0.7)	7.5%	5.3%	**0.572	**0.51 (0.5-0.6)	**0.9%	**−0.9%
GBM-molRPA by Wee et al. (3 groups)***	*0.001	0.60 (0.6-0.6)	7.3%	6.6%	*0.001	0.59 (0.5-0.6)	10.7%	6.3%

Legends:
 IPA: index of prediction accuracy defined as $IPA = 1 - (\text{model Brier score [18 months]} / \text{null model Brier score [18 months]})$
 *The variable 'able to work' was defined with a KPS of 80 and more.
 **The size of the validation cohort for the RPA proposed by Molinaro et al. was only n = 135 due to missing variables on pre- or post-operative tumor volumes. Calculated measurements need therefore to be interpreted with a high level of caution.
 ***No IDH-mutant tumors were included given that the WHO 2021 classification restricted the diagnosis of glioblastoma to IDH-wildtype tumors. Accordingly, RPA class 1 originally including also IDH-mutant tumors was limited in size (exploratory cohort: n = 97; validation cohort: n = 6)

Figure 4. External validation and comparison with other risk models. (A) Schematic representation of the formation of the final validation cohort exclusively including IDH-wildtype glioblastomas in which complete information to calculate the RANO risk score were available (n = 210). (B)–(D) Kaplan–Meier estimates of overall survival for patients in the validation cohort displayed for the overall cohort (B) and for the subgroups of patients treated with postoperative radiochemotherapy (C; TMZ/RT→TMZ; n = 132) or other management approaches (D; n = 78). Note that the presence of three distinct survival groups was confirmed. Points indicate deceased or censored patients, light shading indicates SEM. (E) Goodness-of-fit measurements including Harrell's c-index and pseudo-R² values for the RANO risk score model, the simplified RTOG RPA model, the RPA described by Molinaro and colleagues (2020), and the GBM-molRPA. Measurements were assessed separately for the training (n = 771) and validation cohort (n = 210).

Collectively, we herein introduce the easy-to-use yet highly prognostic “*RANO risk score for postoperative outcome*” to assign glioblastoma patients into distinct categories according to the expected postoperative survival. The model reflects the integration of prognostic markers into a single measurement and aims to serve to reduce imbalances between study arms in the setting of clinical trials.

Supplementary material

Supplementary material is available online at *Neuro-Oncology* (<https://academic.oup.com/neuro-oncology>).

Keywords

extent of resection | glioblastoma | patient stratification | postoperative risk modeling | risk assessment

Acknowledgments

The authors thank all patients who contributed to the results of the study. [Figure 1](#) has been created with the help of BioRender.com. Parts of the study were presented as an abstract at the 2024 Annual Meeting of the American Society for Clinical Oncology (ASCO), selected to receive an ASCO Endowed Conquer Cancer Merit Award in Memory of Joe Hogan, and awarded the Neurosurgery Award 2024 of the Annual Meeting of the Society for Neuro-Oncology (SNO).

Funding

Nothing to report.

Conflict of interest statement. J. Dietrich—Consultant and Advisory Board: Amgen, Novartis, Janssen. Research Support: Ono Therapeutics and Novartis. Royalties: Wolters Kluwer. M. Weller—Research grants: Novartis, Quercis, Versameb. Honoraria or advisory board participation and consulting: Anheart, Bayer, CureVac, Medac, Neurosense, Novartis, Novocure, Orbus, Philogen, Pfizer, Roche, Servier. M. A. Vogelbaum—Indirect equity and patent royalty interests: Infuseon Therapeutics. Honoraria: Chimerix, Midatech. Research grants: DeNovo Pharma, Oncosynergy, Infuseon, Chimerix. M. van den Bent—Consultant: Celgene, Boehringer, Carthera, Nerviano, Genenta, Servier, Anheart Therapeutics, Boehringer Ingelheim, Fore Biotherapeutics, Incyte, Symbiopharma. D. P. Cahill—Advisory: Lilly, GlaxoSmithKline, Incephalo, Boston Pharmaceuticals, Servier, Boston Scientific, Pyramid Biosciences (equity interest). Speaker Honoraria: Merck. Clinical trial and grant review: US NIH and DOD. R. Rudà—Honoraria, advisory board, and consulting: UCB, Bayer, Novocure, Genenta, Servier. P. Y. Wen—Research support:

Astra Zeneca, Black Diamond, Bristol Meyers Squibb, Chimerix, Eli Lilly, Erasca, Global Coalition For Adaptive Research, Kazia, MediciNova, Merck, Novartis, Quadriga, Servier, VBI Vaccines. Advisory Board/consultant: Anheart, Astra Zeneca, Black Diamond, Celularity, Chimerix, Day One Bio, Genenta, Glaxo Smith Kline, Kintara, Merck, Mundipharma, Novartis, Novocure, Prelude Therapeutics, Sagimet, Sapience, Servier, Symbio, Tango, Telix, VBI Vaccines. R. Y. Huang—Advisory board: Vysioneer. Consulting: Nuvation Bio. J.-C. Tonn—Research grants: Novocure, Munich Surgical Imaging. Consultant: AAA Novartis, Servier. Royalties: Springer Publisher. P.K., J.C.Y., G.C.Y., A.D., L.H., T.S., F.B., S.T.J., N.Te., J.B., N.Th., J.K.W.G., S.H.J., D.P.C., S.M.C., L.B., O.S., Y.E., M.I.R., S.J.G., A.M.M., M.S.B.—None.

Author contributions

Study concept and design: P.K., A.M.M., and J.C.T. Data collection: P.K., J.S.Y., G.C.Y., A.D., L.H., T.S., F.B., S.T.J., N.Te., J.D., and R.Y.H. Data analysis and interpretation: P.K., J.D., M.W., M.A.V., M.v.d.B., A.M.M., S.M.C., and J.C.T. Manuscript drafting: P.K., J.C.T. Manuscript revising: P.K., J.S.Y., G.C.Y., A.D., L.H., T.S., F.B., S.T.J., N.Te., J.D., M.W., M.A.V., M.v.d.B., J.B., N.Th., J.K.W.G., S.H.J., D.P.C., S.M.C., R.R., L.B., O.S., Y.E., M.I.R., S.J.G., R.Y.H., P.Y.W., M.S.B., A.M.M., and J.C.T.

Affiliations

Department of Neurosurgery, LMU University Hospital of the Ludwig-Maximilians-University Munich, Munich, Germany (P.K., N.Teske, N.Thon, J.-C.T.); Department of Neurosurgery, FAU University Hospital of the Friedrich-Alexander-University, Erlangen, Germany (P.K., N.Teske, O.S.); Department of Neurosurgery & Division of Neuro-Oncology, University of San Francisco, San Francisco, California, US (J.S.Y., J.K.W.G., S.H.-J., S.M.C., M.S.B., A.M.M.); Center for Neuro-Oncology, Dana-Farber Cancer Institute and Harvard Medical School, Boston, Massachusetts, US (G.C.Y., P.Y.W.); Department of Neurosurgery, McGovern Medical School at UT Health Houston, Houston, Texas, US (A.D., Y.E.); Department of Neurosurgery, Medical Center - University of Freiburg, Freiburg, Germany (L.H., J.B., O.S.); Department of Neurosurgery, Inselspital, Bern University Hospital, and University of Bern, Bern, Switzerland (L.H.); Division of Neuro-Oncology, Department of Oncology and Hemato-Oncology, University of Milan, Milan, Italy (T.S., L.B.); Division of Neuro-Oncology, Department of Neurosciences, University of Turin, Italy (F.B., R.R.); Department of Neurosurgery, University of Cologne, Cologne, Germany (S.T.J., S.J.G.); Division of Neuro-Oncology, Department of Neurology, Massachusetts General Hospital Cancer Center, Harvard Medical School, Boston, Massachusetts, US (J.D.); Department of Neurology, University Hospital and University of Zurich, Zurich, Switzerland (M.W.); Department of NeuroOncology, Moffitt Cancer Center, Tampa, Florida, US (M.A.V.); Department of Neurology, Erasmus MC Cancer Institute, Rotterdam, The Netherlands (M.B.); Department of Neurosurgery, Erasmus MC Cancer Institute, Rotterdam, The Netherlands (J.K.W.G.); Department of Neurosurgery, Massachusetts General Hospital,

Harvard Medical School, Boston, Massachusetts, US (D.P.C.); Department of Stereotactic and Functional Neurosurgery, Centre of Neurosurgery, University of Cologne, Cologne, Germany (M.I.R.); Klinikum Fulda, Academic Hospital of Marburg University, Fulda, Germany (S.J.G.); Division of Neuroradiology, Brigham and Women's Hospital and Harvard Medical School, Boston, Massachusetts, US (R.Y.H.); German Cancer Consortium (DKTK), Partner Site Munich, Munich, Germany (J.-C.T.)

References

- Ostrom QT, Price M, Neff C, et al. CBTRUS statistical report: primary brain and other central nervous system tumors diagnosed in the United States in 2015-2019. *Neuro Oncol*. 2022;24(Suppl 5):v1-v95.
- Weller M, van den Bent M, Preusser M, et al. EANO guidelines on the diagnosis and treatment of diffuse gliomas of adulthood. *Nat Rev Clin Oncol*. 2021;18(3):170-186.
- Wen PY, Weller M, Lee EQ, et al. Glioblastoma in adults: a Society for Neuro-Oncology (SNO) and European Society of Neuro-Oncology (EANO) consensus review on current management and future directions. *Neuro Oncol*. 2020;22(8):1073-1113.
- Karschnia P, Smits M, Reifenberger G, et al.; Expert Rater Panel. A framework for standardised tissue sampling and processing during resection of diffuse intracranial glioma: joint recommendations from four RANO groups. *Lancet Oncol*. 2023;24(11):e438-e450.
- Karschnia P, Dono A, Young JS, et al. Prognostic evaluation of re-resection for recurrent glioblastoma using the novel RANO classification for extent of resection: a report of the RANO resect group. *Neuro Oncol*. 2023;25(9):1672-1685.
- Rahman R, Polley MC, Alder L, et al. Current drug development and trial designs in neuro-oncology: report from the first American Society of Clinical Oncology and Society for Neuro-Oncology Clinical Trials Conference. *Lancet Oncol*. 2023;24(4):e161-e171.
- Singh K, Hotchkiss KM, Parney IF, et al. Correcting the drug development paradigm for glioblastoma requires serial tissue sampling. *Nat Med*. 2023;29(10):2402-2405.
- Molinaro AM, Hervey-Jumper S, Morshed RA, et al. Association of maximal extent of resection of contrast-enhanced and non-contrast-enhanced tumor with survival within molecular subgroups of patients with newly diagnosed glioblastoma. *JAMA Oncol*. 2020;6(4):495.
- Gerritsen JKW, Zwarthoed RH, Kilgallon JL, et al. Effect of awake craniotomy in glioblastoma in eloquent areas (GLIOMAP): a propensity score-matched analysis of an international, multicentre, cohort study. *Lancet Oncol*. 2022;23(6):802-817.
- Karschnia P, Young JS, Dono A, et al. Prognostic validation of a new classification system for extent of resection in glioblastoma: a report of the RANO resect group. *Neuro Oncol*. 2023;25(5):940-954.
- Gerritsen JKW, Zwarthoed RH, Kilgallon JL, et al. Impact of maximal extent of resection on postoperative deficits, patient functioning, and survival within clinically important glioblastoma subgroups. *Neuro Oncol*. 2023;25(5):958-972.
- Louis DN, Perry A, Wesseling P, et al. The 2021 WHO Classification of Tumors of the Central Nervous System: a summary. *Neuro Oncol*. 2021;23(8):1231-1251.
- Karschnia P, Dietrich J, Bruno F, et al. Surgical management and outcome of newly diagnosed glioblastoma without contrast enhancement ('low grade appearance')—a report of the RANO resect group. *Neuro Oncol*. 2023.
- Vogelbaum MA, Jost S, Aghi MK, et al. Application of novel response/progression measures for surgically delivered therapies for gliomas: Response Assessment in Neuro-Oncology (RANO) Working Group. *Neurosurgery*. 2012;70(1):234-243; discussion 243.
- Wen PY, Macdonald DR, Reardon DA, et al. Updated response assessment criteria for high-grade gliomas: response assessment in neuro-oncology working group. *J Clin Oncol*. 2010;28(11):1963-1972.
- Youssef G, Rahman R, Bay C, et al. Evaluation of standard response assessment in neuro-oncology, modified response assessment in neuro-oncology, and immunotherapy response assessment in neuro-oncology in newly diagnosed and recurrent glioblastoma. *J Clin Oncol*. 2023;41(17):3160-3171.
- van Putten W. CART: Stata module to perform Classification And Regression Tree analysis. *Boston College Department of Economics*. 2006:S456776.
- Elith J, Leathwick JR, Hastie T. A working guide to boosted regression trees. *J Anim Ecol*. 2008;77(4):802-813.
- Perry JR, Laperriere N, O'Callaghan CJ, et al.; Trial Investigators. Short-course radiation plus temozolomide in elderly patients with glioblastoma. *N Engl J Med*. 2017;376(11):1027-1037.
- Osterman CK, Sanoff HK, Wood WA, Fasold M, Lafata JE. Predictive modeling for adverse events and risk stratification programs for people receiving cancer treatment. *JCO Oncol Pract*. 2022;18(2):127-136.
- Kattan MW, Gerds TA. The index of prediction accuracy: an intuitive measure useful for evaluating risk prediction models. *Diagn Progn Res*. 2018;2:7.
- Linden A, Gerds TA, Huber C. STBRIER: Stata module to compute Brier score for censored time-to-event (survival) data. *Stata J*. 2017.
- Stupp R, Hegi ME, Mason WP, et al.; European Organisation for Research and Treatment of Cancer Brain Tumour and Radiation Oncology Groups. Effects of radiotherapy with concomitant and adjuvant temozolomide versus radiotherapy alone on survival in glioblastoma in a randomised phase III study: 5-year analysis of the EORTC-NCIC trial. *Lancet Oncol*. 2009;10(5):459-466.
- Li J, Wang M, Won M, et al. Validation and simplification of the Radiation Therapy Oncology Group recursive partitioning analysis classification for glioblastoma. *Int J Radiat Oncol Biol Phys*. 2011;81(3):623-630.
- Wee CW, Kim E, Kim N, et al. Novel recursive partitioning analysis classification for newly diagnosed glioblastoma: a multi-institutional study highlighting the MGMT promoter methylation and IDH1 gene mutation status. *Radiother Oncol*. 2017;123(1):106-111.
- Ostrom QT, Price M, Neff C, et al. CBTRUS Statistical Report: primary brain and other central nervous system tumors diagnosed in the United States in 2016-2020. *Neuro Oncol*. 2023;25(12 Suppl 2):iv1-iv99.
- Ostrom QT, Shoaf ML, Cioffi G, et al. National-level overall survival patterns for molecularly-defined diffuse glioma types in the United States. *Neuro Oncol*. 2023;25(4):799-807.
- Roder C, Stummer W, Coburger J, et al. Intraoperative MRI-guided resection is not superior to 5-aminolevulinic acid guidance in newly diagnosed glioblastoma: a prospective controlled multicenter clinical trial. *J Clin Oncol*. 2023;41(36):5512-5523.
- Stummer W, Reulen HJ, Meinel T, et al.; ALA-Glioma Study Group. Extent of resection and survival in glioblastoma multiforme: identification of and adjustment for bias. *Neurosurgery*. 2008;62(3):564-576; discussion 564.
- Bjorland LS, Mahesparan R, Fluge O, et al. Impact of extent of resection on outcome from glioblastoma using the RANO resect group classification system: a retrospective, population-based cohort study. *Neurooncol*. 2023;5(1):v126.
- Karschnia P, Vogelbaum MA, van den Bent M, et al. Evidence-based recommendations on categories for extent of resection in diffuse glioma. *Eur J Cancer*. 2021;149:23-33.

32. Tropeano MP, Raspagliesi L, Bono BC, et al. Supramaximal resection: retrospective study on IDH-wildtype glioblastomas based on the new RANO-resect classification. *Acta Neurochir (Wien)*. 2024;166(1):196.
33. Hegi ME, Genbrugge E, Gorlia T, et al. MGMT promoter methylation cutoff with safety margin for selecting glioblastoma patients into trials omitting temozolomide: a pooled analysis of four clinical trials. *Clin Cancer Res*. 2019;25(6):1809–1816.
34. Wick W, Platten M, Meisner C, et al.; NOA-08 Study Group of Neuro-oncology Working Group (NOA) of German Cancer Society. Temozolomide chemotherapy alone versus radiotherapy alone for malignant astrocytoma in the elderly: the NOA-08 randomised, phase 3 trial. *Lancet Oncol*. 2012;13(7):707–715.
35. Cahill DP, Dunn GP. Considering the extent of resection in diffuse glioma. *Neuro Oncol*. 2023;25(12):2134–2135.
36. Aabedi AA, Young JS, Zhang Y, et al. Association of neurological impairment on the relative benefit of maximal extent of resection in chemoradiation-treated newly diagnosed isocitrate dehydrogenase wild-type glioblastoma. *Neurosurgery*. 2022;90(1):124–130.
37. Laigle-Donadey F, Metellus P, Guyotat J, et al. Surgery for glioblastomas in the elderly: an Association des Neuro-oncologues d'Expression Française (ANOCEF) trial. *J Neurosurg*. 2023;138(5):1199–1205.
38. Drexler R, Schüller U, Eckhardt A, et al. DNA methylation subclasses predict the benefit from gross total tumor resection in IDH-wildtype glioblastoma patients. *Neuro Oncol*. 2023;25(2):315–325.
39. Nayak L, DeAngelis LM, Brandes AA, et al. The Neurologic Assessment in Neuro-Oncology (NANO) scale: a tool to assess neurologic function for integration into the Response Assessment in Neuro-Oncology (RANO) criteria. *Neuro Oncol*. 2017;19(5):625–635.